

## Eco-Friendly Synthesis and Characterization of Silver and Zinc Nanoparticles Using Aqueous Extract from the Bark of *Antiaris toxicaria*

Thomas Ndidi Asiwe, Idongesit Bassey Anweting\*, Atim Sunday Johnson, Nzikahyel Simon and Solomon Enejo Shaibu

Received: 12 September 2024/Accepted 03 December 2024/published: 05 December 2024

**Abstract:** Silver nanoparticles (AgNPs) and zinc nanoparticles (ZnNPs) were synthesized by a cheap, rapid, and eco-friendly method using aqueous bark extract of *Antiaris toxicaria* as both the reducing and capping agents. The synthesized AgNPs and ZnNPs were characterized using a UV-visible spectroscopy, Fourier Transform infrared spectroscopy (FTIR), Transmission electron microscopy (TEM), Scanning electron microscopy (SEM), X-ray diffraction (XRD), and Energy dispersive spectroscopy (EDS). The metal ions ( $M^+$ ) were rapidly reduced from  $M^+$  to  $M^0$  by the aqueous bark extract of *Antiaris toxicaria*, forming AgNPs and ZnNPs with sizes ranging between 1- 100 nm. The diffraction peaks were indexed to the face-centered cubic (fcc) phase of silver and zinc, indicating that the synthesized AgNPs and ZnNPs were crystalline in nature. Absorption spectra of AgNPs and ZnNPs showed a surface plasmon resonance (SPR) peak around a wavelength of 423 nm and 306 nm respectively. The FTIR spectra revealed distinct peaks at  $3295.38\text{ cm}^{-1}$  attributed to the OH group which may be responsible for the reduction of  $M^+$  to  $M^0$  and subsequent formation of metal MNPs,  $2104.38\text{ cm}^{-1}$  corresponding to asymmetric stretching vibrations of methylene ( $\text{CH}_2$ ) group in AgNPs, and a sharp peak at  $1634.80\text{ cm}^{-1}$  corresponding to a carbonyl ( $\text{C}=\text{O}$ ) group.

**Keywords:** Silver nanoparticles, zinc nanoparticles, *Antiaris toxicaria*, characterization, plant extract

**Thomas Ndidi Asiwe**

Department of Chemistry, Faculty of Physical Sciences, University of Uyo, Uyo, Nigeria

Email: [michaelasiwe@gmail.com](mailto:michaelasiwe@gmail.com)

**Idongesit Bassey Anweting\***

Department of Chemistry, Faculty of Physical Sciences, University of Uyo, Uyo, Nigeria

Email: [idongesitanweting@uniuyo.edu.ng](mailto:idongesitanweting@uniuyo.edu.ng)

Orcid id: 0000-0002-9251-3991

**Atim Sunday Johnson**

Department of Chemistry, Faculty of Physical Sciences, University of Uyo, Uyo, Nigeria

Email: [atimjohnson@uniuyo.edu.ng](mailto:atimjohnson@uniuyo.edu.ng)

Orcid id: 0000-0001-8732-2704

**Nzikahyel Simon**

Department of Chemistry, Faculty of Physical Sciences, University of Uyo, Uyo, Nigeria

Email: [nzikahyelsimon@uniuyo.edu.ng](mailto:nzikahyelsimon@uniuyo.edu.ng)

Orcid id: 0000-0001-8732-2704

**Solomon Enejo Shaibu**

Department of Chemistry, Faculty of Physical Sciences, University of Uyo, Uyo, Nigeria

Email: [shaibusolomon@uniuyo.edu.ng](mailto:shaibusolomon@uniuyo.edu.ng)

Orcid id: 0000-0002-6753-7633

### 1.0 Introduction

The increasing demand for environmentally friendly and non-toxic approaches to synthesizing metal nanoparticles has led to significant advancements in bio-reduction processes using plant materials. Unlike traditional chemical methods, which often involve toxic and hazardous reactants, green synthesis leverages phytochemicals in plants to act as reducing and capping agents. These phytochemicals, including flavonoids, tannins,

phenols, saponins, terpenoids, and glycosides, facilitate the reduction of metal ions to zero-valent metal nanoparticles and stabilize them without introducing harmful byproducts (Harun-Ur-Rashid *et al.*, 2023; Sharma *et al.*, 2021; Banjara *et al.*, 2024; Gopalakrishnan *et al.*, 2015). The advantages of this approach—eco-friendliness, cost-effectiveness, and operation under mild conditions—make it superior to conventional chemical and physical methods (Ying *et al.*, 2022; Ekwumemgbo *et al.*, 2023; Kpega *et al.*, 2023; Afonso *et al.*, 2024).

The bark of *Antiaris toxicaria*, a tropical forest tree native to regions like Nigeria, Kenya, and Sudan, represents a promising bio-resource for this purpose. Traditionally, *A. toxicaria* has been used in the treatment of syphilis, chest pains, seizures, chronic tremors, and mental disorders, owing to its rich phytochemical composition (Richards *et al.*, 2021). These bioactive compounds, including alkaloids, flavonoids, phenols, and saponins, make *A. toxicaria* an excellent candidate for the green synthesis of nanoparticles (Gopalakrishnan *et al.*, 2015; Shreyash *et al.*, 2021).

Silver and zinc nanoparticles (AgNPs and ZnNPs) synthesised using plant extracts are of particular interest due to their unique properties and wide-ranging applications (Fahim *et al.*, 2024; Garg *et al.*, 2022; Odoemelam *et al.*, 2023). AgNPs are extensively used in bioremediation, antimicrobial activities, and catalysis (Akpanudo and Olabimewo, 2024), while ZnNPs are prized for their large surface area, high reactivity, and electrical and magnetic properties, making them suitable for biomedical, electronic, and catalytic applications (Sharma *et al.*, 2022; Nair *et al.*, 2022). Some literature have reported the successful synthesis of AgNPs using various plant extracts. For example, Alex *et al.* (2024) produced AgNPs using *Ocimum sp* as a reducing agent. The product was further tested and confirmed to be effective as an anticancer agent. Hossain *et al.*, (2024) observed good

microbial activity of AgNPs, synthesised from the microextract of *Phyllanthus emblica*, which showed up to 70% purity. The products were also characterised using XRD, SEM, TEM and FTIR and found to be active in several microorganisms. The work published by Akpanudo and Olabemiwo (2024) also reported the use of AgNPs synthesised with *Echinochloa pyramidalis* as adsorbent for the removal of polyaromatic hydrocarbons. Also, AgNPs, produced from extract of *Aloe fleurentinorum* was found to exhibit a significant antibacterial activity. Also, ZnNPs obtained from plant mediated approach have shown some functionality and broader application scope such as application in water purification (Odoemelam *et al.*, 2023), antibacterials and antioxidant activities (Islam *et al.*, 2024), antiskin cancer, antimicrobial and antioxidant activities (Naiel *et al.*, 2022)

Several studies on the synthesis of zinc and silver nanoparticles have been reported, especially those involving the use of plant extracts. However, most of the studies concentrate on the use of a particular plant for a given metal nanoparticles, without considering multi-dimensional approaches. A report of the investigation carried out by Punjabi *et al.* (2024) indicated that a given plant extract can be useful in the synthesis of both zinc and silver nanoparticles. In their study, they used *Pseudomonas hibiscicola* to reduce the corresponding metal salts. To the knowledge of the authors, no such studies have been reported on the use of aqueous extract of *Antiaris Toxicaria* bark for the synthesis of AgNPs or ZnNPs or both. Regarding the need to bridge this knowledge gap and to contribute to research data, the present study aims to utilize the aqueous extract of *A. toxicaria* bark as a reducing and capping agent for the green synthesis of AgNPs and ZnNPs. Comprehensive characterization of the synthesized nanoparticles will be performed using techniques such as UV-visible spectroscopy (UV-Vis), Fourier Transform



Infrared Spectroscopy (FTIR), X-ray Powder Diffraction (XRD), and Transmission Electron Microscopy (TEM).

This study is justified by its potential to enhance the understanding and application of sustainable nanotechnology. The eco-friendly synthesis of AgNPs and ZnNPs using *A. toxicaria* not only aligns with green chemistry principles but also offers an innovative approach to utilizing an underexplored natural resource. Furthermore, exploring the potential of *A. toxicaria* in nanoparticle synthesis could lead to significant contributions in environmental remediation, biomedicine, and materials science, addressing both scientific and societal needs.

## 2.0 Materials and Methods

### 2.1 Materials

Silver nitrate ( $\text{AgNO}_3$ ) SureChem product (97.0% pure), zinc chloride ( $\text{ZnCl}_2$ ) SureChem product (97.0% pure). All reagents used in this study were of analytical grade and were obtained from commercial sources. Deionized distilled water was used throughout the experiments. *Antiaris toxicaria* were collected from Ibiono Local Government Area of Akwa Ibom State, Nigeria.

### 2.2 Preparation of extract

The bark of *Antiaris toxicaria* was washed thoroughly with tap water and then with deionized water. It was cut into pieces and air-dried. The dried bark of *A. toxicaria* was granulated into powder form. 30g of the ground bark of *A. toxicaria* was weighed out using a weighing balance into a 500 mL Erlenmeyer flask and 300 mL of deionized water was added into the flask and mix. The mixture was boiled for about 30 minutes at 80 °C and allowed to cool and filtered with Whatman No.1 filter paper. The filtrate was used as the extract in the synthesis of the metal nanoparticles.

### 2.3 Synthesis of metal nanoparticles

The synthesis of AgNPs and ZnNPs were carried out according to Essien *et al.* (2020)

with little modification, it involved the use of silver nitrate ( $\text{AgNO}_3$ ) and  $\text{ZnCl}_2$  respectively as the precursors while freshly prepared plant extract was used as a reducing and stabilizer agent. Solutions of 0.001 M ( $\text{AgNO}_3$ ) and 0.001M ( $\text{ZnCl}_2$ ) were prepared by adding 0.043 g of solid  $\text{AgNO}_3$  and 0.034 g of solid  $\text{ZnCl}_2$  respectively in 250 mL deionized water and stirred. The aqueous solution containing the precursors were heated in a hot plate set at 60 °C for 5 min, under constant stirring. For the green synthesis of AgNPs and ZnNPs nanoparticles, 5 mL of the plant extract was respectively added to 5 mL of 0.001 M  $\text{AgNO}_3$  and 0.001M  $\text{ZnCl}_2$  precursors solution with continuous stirring for a for a homogeneous reaction. When the extract was added to the AgNPs precursor the colour of the resulting homogeneous solution changed gradually from light brown to brick red while ZnNPs changed from light brown to deep brown.

The nanoparticles formed were filtered using Whatman filter paper No. 1 and subsequently washed using deionized water. The dried precipitate was oven dried at 70 °C for 2 h and stored in a seal-tight container for further use.

### 2.4 Characterization of synthesized nanoparticles

UV-Visible spectral analysis was carried out using a Shimadzu UV-visible spectrophotometer (UV-1800, Japan). UV-visible absorption spectrophotometer with a resolution of 1 nm between 200 and 800 nm was used. One milliliter of the sample was pipetted into a test tube and subsequently analyzed at room temperature. FT-IR spectra were recorded on a Perkin Elmer 1750 FTIR Spectrophotometer. Elemental composition and stoichiometry of the sample were analyzed with energy dispersive analysis of X-ray spectroscopy (EDS) coupled to the scanning electron microscope (SEM) JEOL JSM – 6610 LV. The particle size and surface morphology were analyzed using Transmission electron microscopy (TEM), and images were recorded



on JEOL instrument JEM – 2100 F instrument on carbon-coated copper with an accelerating voltage of 200Kv. Scanning Electron Microscopy (SEM) images were recorded on JEOL instrument JSM – 6610LV. X-ray diffraction (XRD) analysis was recorded on an Ultima IV X-ray Diffractometer (Rigaku, Japan) in the range 2 theta 4 deg to 90 deg at a scan rate of 2 degrees/min. Catalytic activity of the synthesized silver nanoparticles was evaluated using a Unicam Helios spectrophotometer.

### 3.0 Results and Discussion

The reduction of silver nitrate and zinc chloride into AgNPs and ZnNPs respectively upon mixing with the plant extract in 1 :1 ratio was indicated by a gradual colour change within 60 minutes of mixing. This might be as a result of the excitation of the surface Plasmon resonance (SPR) of the synthesized silver nanoparticles (Adrianto *et al.*, 2022; Juma *et al.*, 2024). These characteristic color variations are due to the formation of AgNPs and ZnNPs. This reduction is as a result of the phenolic compounds and secondary metabolites present in the plant extract. These phytochemicals in plant extracts possess redox properties that

facilitate the reduction of metal precursors and subsequent change into their corresponding metallic nanoparticles (Adeyemi *et al.*, 2022). *A. toxicaria* extract contains flavonoids, alkaloids, tannins, terpenoids, phenols, saponins, and glycosides, (Subiono & Tavip, 2023; Alsailawi *et al.*, 2023).

#### 3.1 UV-visible spectroscopy analysis of the green synthesized AgNPs and ZnNPs

The UV-Visible spectroscopy is one of the most important and widely used simple and sensitive techniques for determining the formation of metal nanoparticles (Ahmed *et al.*, 2022). UV-Visible spectra of the AgNPs and ZnNPs are presented in Fig. 1a and b. The absorbance maximum was observed around a wavelength of 423 nm for AgNPs and 306 nm for ZnNPs, which is characteristic of silver and zinc surface plasmon resonance (SPR). The results indicate that AgNPs absorb in the visible region while the ZnNPs absorb in the ultra violet region. This results agrees with some literature values such as 405 nm (Anandalakshmi *et al.*, 2016) and 450 nm (Jose *et al.*, 2022) reported for AgNPs as well as 367 nm (Sing *et al.*, 2023) and 300 nm (Saputra & Yulizar, 2016) for ZnNPs.

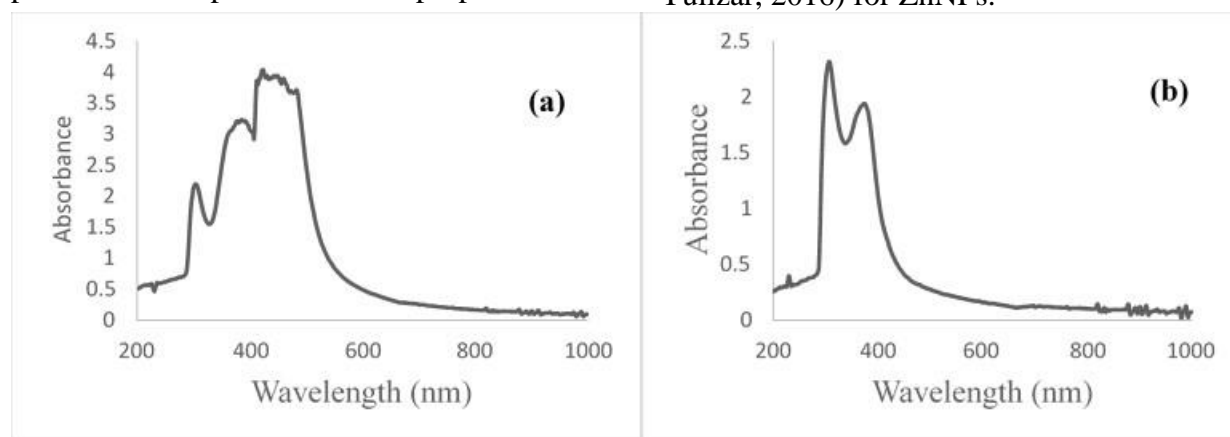


**Fig. 1.** UV-visible spectrum of (a) AgNPs and (b) ZnNPs synthesized using *A. toxicaria* bark aqueous extract.

The wavelength of maximum absorption can also be linked to the bandgap using the Planck equation given below (Eddy *et al.*, 2024a-n)

$$E_{BG} = \frac{hc}{\lambda_{max}} \quad (1)$$

where  $E_{BG}$  is the band gap in eV,  $h$  is the Planck constant, and  $c$  is the speed of light. Consequently, we calculated the band gap of AgNPs and ZnNPs as 2.93 eV and 4.05 nm. This implies that it requires less energy to



create hole in the valence band and electrons in the conduction band of AgNPs than in ZnNPs. This also suggests that AgNPs can be a better photocatalyst than ZnNPs (Eddy *et al.*, 2023a-c)

The phytochemical analysis of *A. toxicaria* reveals the presence of flavonoids, alkaloids, steroids, rosins, saponins, and proteins (Subiono, & Tavip, 2023; Alsailawi *et al.* 2023). In bark extract (Fig. 2a), the peaks are

observed at 402.66, 413.97, 422.29, 467.28, 567.06, 1635.41, and 3325.35  $\text{cm}^{-1}$ , respectively.

### 3.2 Fourier transform-infrared radiation (FT-IR) analysis

FTIR measurements were carried out to identify the possible biomolecules in the *A. toxicaria* extract. FTIR spectra of aqueous extract and synthesized AgNPs and ZnNPs are shown in Fig. 2a, 2b, and 2c respectively.

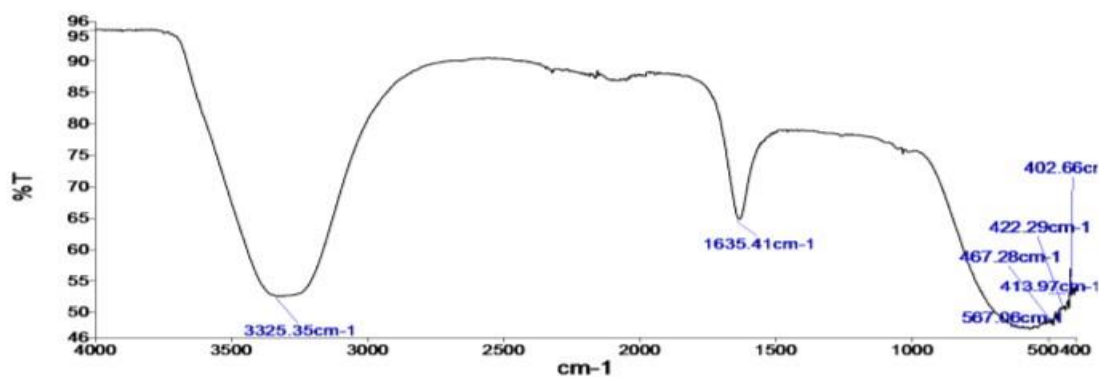


Fig. 2a. FT-IR spectrum of *A. toxicaria* extract.

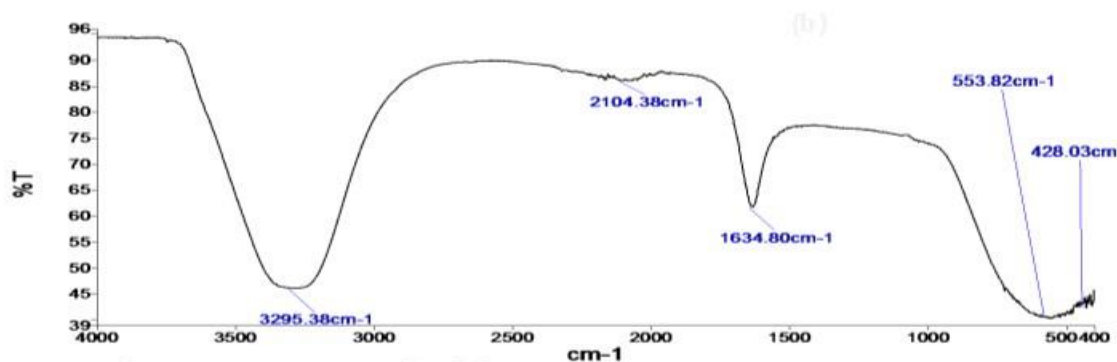


Fig. 2b. FT-IR spectrum of synthesized AgNPs

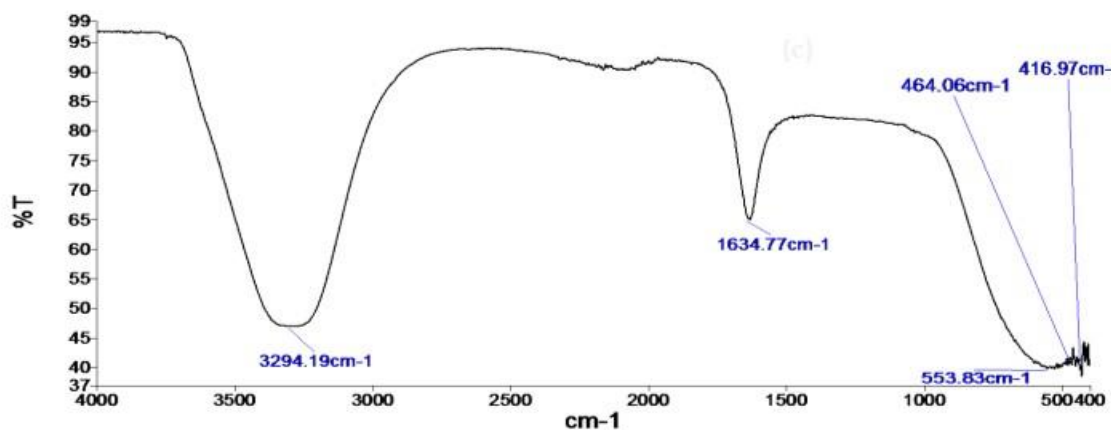


Fig. 2c. FT-IR spectrum of synthesized ZnNPs



With  $\text{AgNO}_3$  in Fig. 2b, the peaks were shifted to a higher wave number side, such as 428.03, 553, 1634.80, 2104.38, and 3295.38  $\text{cm}^{-1}$ . The peak at 402.66  $\text{cm}^{-1}$  of the extract is shifted toward a higher wave number side at 428.03  $\text{cm}^{-1}$  due to the O–Ag–O network and ring opening vibration. The band observed at 567.06  $\text{cm}^{-1}$  is shifted to the lower side at 553  $\text{cm}^{-1}$ , which corresponds to C–Cl stretching in the alkyl group. The very strong band at 1634.80  $\text{cm}^{-1}$  is due to C=C stretching in the aromatic ring, confirming the presence of the aromatic group and the band at 2104.38 is due to methylene group  $\text{CH}_2$  and C–H alkane groups (Pungle *et al.*, 2023). The silver nanoparticles of O–H stretching in carboxylic acids vibration is shifted from 3325.35 to 3295.38  $\text{cm}^{-1}$ . In the same trend with zinc chloride Fig. 2c, the peaks observed in the *A. toxicaria* were also shifted towards higher wave number sides at 416.97  $\text{cm}^{-1}$ , 464.06  $\text{cm}^{-1}$  due to its ring-opening vibration. The band observed at 567.06  $\text{cm}^{-1}$  is shifted to the lower side at 553.83  $\text{cm}^{-1}$ , which corresponds to C–Cl stretching in the alkyl group. The very strong band at 1634.77  $\text{cm}^{-1}$  is due to C=C stretching in the aromatic ring, confirming the presence of the aromatic group. The O–H stretching in carboxylic acids vibration is shifted from 3325.35 to 3294.19  $\text{cm}^{-1}$ . The immediate reduction and capping of silver ions and zinc ions into silver and zinc nanoparticles in the present analysis might be due to flavonoids and proteins. The flavonoids present in the leaf extract are powerful reducing agents which may be suggestive of the formation of AgNPs and ZnNPs by reduction of silver nitrate and zinc chloride. The flavonoid compounds in the water extract of *A. toxicaria* might be actively involved and responsible for the reduction of  $\text{M}^+$  to  $\text{M}^0$  (Anandalakshmi *et al.*, 2016). The involvement of water-soluble flavonoids in the reduction of metal ions using plant extracts is also evidenced in another study (Rahman *et al.*, 2024).

### 3.3 Morphological analysis

The SEM and TEM images for both silver nanoparticles (AgNPs) and zinc nanoparticles (ZnNPs) shown in Fig. 3 reveal key characteristics of their morphology and structure. The SEM image of AgNPs shows noticeable agglomeration, where the nanoparticles are grouped together, forming larger clusters. These particles are predominantly spherical, but their sizes and spacing are irregular. This indicates that the AgNPs have a tendency to agglomerate, likely due to insufficient stabilization during synthesis. In contrast, the SEM image of ZnNPs shows a more dispersed distribution of particles, with some spherical shapes evident, though there is still some degree of agglomeration. The ZnNPs appear to have a more uniform distribution compared to the AgNPs, suggesting better stabilization or slightly different synthesis conditions.

In the TEM images, the AgNPs appear as well-defined spherical particles within the range of 20-100 nm, although the size distribution is not perfectly uniform. Some degree of agglomeration is still visible, indicating that the nanoparticles are loosely clustered, likely due to the synthesis process. On the other hand, the TEM image of ZnNPs reveals a greater variation in particle shape, with both spherical and irregular, elongated particles visible. The size of the ZnNPs is also within the 20-100 nm range, but the particles show more diversity in morphology compared to the AgNPs, which are predominantly spherical. This difference in shape may be attributed to the interaction of the plant extract with the zinc precursor during the synthesis, which may promote more diverse particle formation. When comparing the two sets of nanoparticles, both show similar size ranges, but the AgNPs tend to be more spherical and uniform, while the ZnNPs exhibit a broader variety of shapes, including irregular and elongated ones.



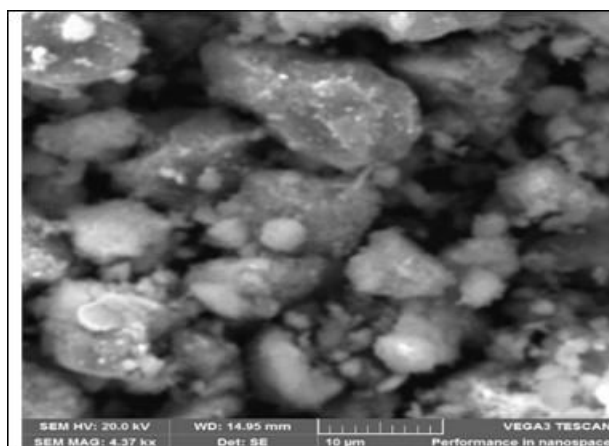


Fig. 3a SEM image of AgNPs

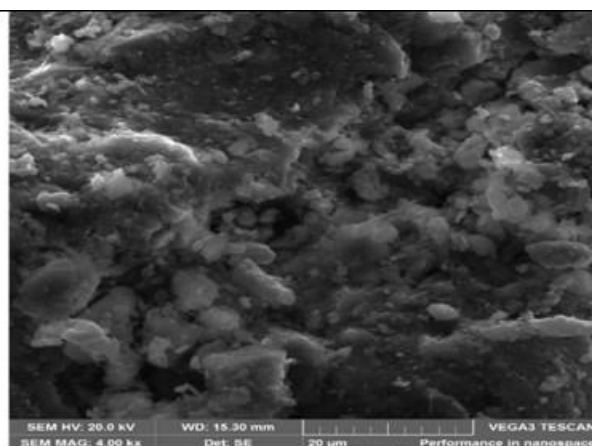


Fig. 3b SEM image of ZnNPs

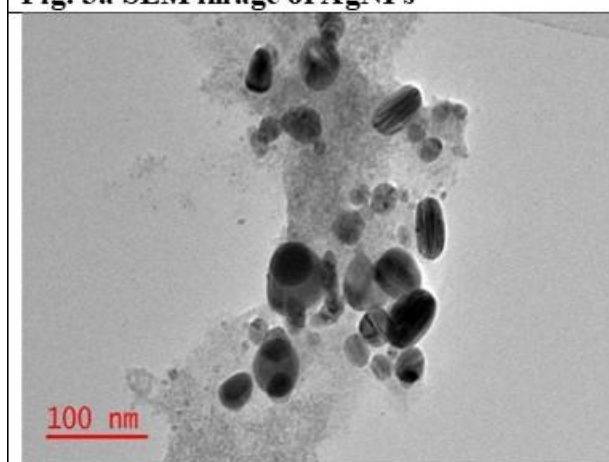


Fig. 3c. TEM image of AgNPs

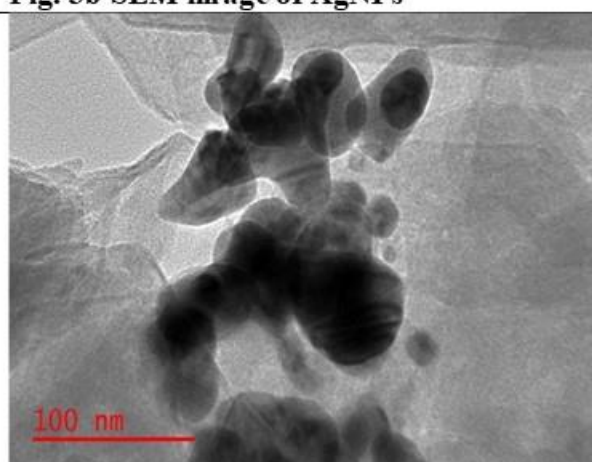


Fig. 3d. TEM image of ZnNPs.

Also, both nanoparticles show some level of agglomeration in the SEM images, but the AgNPs form denser clusters, while the ZnNPs are more evenly distributed. The differences in shape and distribution of the particles can be attributed to the varying effects of the plant extract in stabilizing the nanoparticles during synthesis. The overall morphology suggests that silver nanoparticles tend to form more compact aggregates, whereas zinc nanoparticles maintain a less agglomerated structure with greater variation in particle shape.

### 3.4 Crystallographic analysis

The nanoparticles synthesized using *A. toxicaria* were characterized using powder XRD to confirm the particles as silver and zinc and to know the structural information. Fig 4a

and 4b show the XRD pattern of silver and zinc nanoparticles respectively. The pattern clearly shows the main peaks at  $(2\theta)$   $38.20^\circ$ ,  $44.24^\circ$ , and  $64.30^\circ$  corresponding to the (111), (200), and (220) planes, respectively. By comparing JCPDS (file no: 89-3722), the typical pattern of green-synthesized AgNPs is found to possess an fcc structure. The average crystalline size of the silver nanoparticles was estimated using the Debye–Scherrer's equation (Ali *et al.* 2023):  $D = 0.9\lambda/\beta \cos \theta$ . By determining the width of (111) Bragg's reflection, the estimated average size of the particle is 14 nm. Similar result was observed by Awwad *et al.*, (2020) and Anandalakshmi *et al.*, (2016), who identified crystalline peaks ( $32.28^\circ$ ,  $46.28^\circ$ ,  $54.83^\circ$ ,  $67.47^\circ$  and  $76.69^\circ$ ) which were also obvious in a lot of works in which the XRD pattern included the relevant  $2^\circ$  range. Appearances of these peaks are due to the



presence of phytochemical compounds in the leaf extracts. The stronger planes indicate silver as a major constituent in biosynthesis.

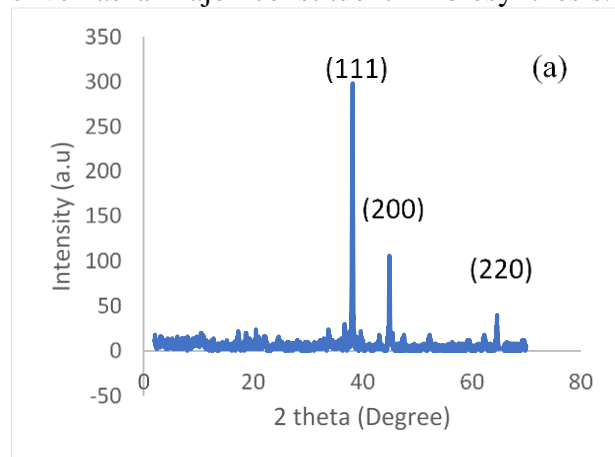


**Fig. 4a: XRD pattern of AgNPs**

### 3.5 Compositional analysis with Energy dispersive spectroscopy (EDS)

The EDS profile for the reduction in Fig. 5a and 5b give additional evidence for the reduction of  $\text{AgNO}_3$  and  $\text{ZnCl}_2$  to elemental silver and zinc respectively. The EDS results for AgNPs (silver nanoparticles) reveal that the major compositions are silver (46.9 wt%), carbon (29.3 wt%), and oxygen (22.1 wt%), with a trace amount of iron (1.7 wt%). The high percentage of silver

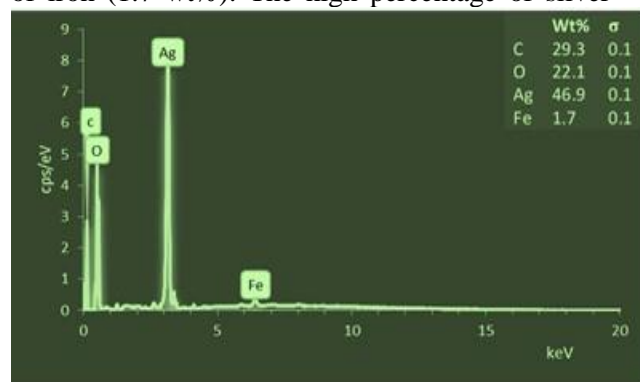


**Fig. 5a: EDS of AgNPs**

The zinc peak confirms the formation of ZnNPs, while the significant proportions of carbon and oxygen suggest surface functionalization with organic molecules or partial oxidation of ZnNPs to zinc oxide (ZnO) during synthesis. Compared to AgNPs, ZnNPs exhibit a higher carbon content,

The observations from the XRD analysis can very well be correlated with the values obtained from TEM images.

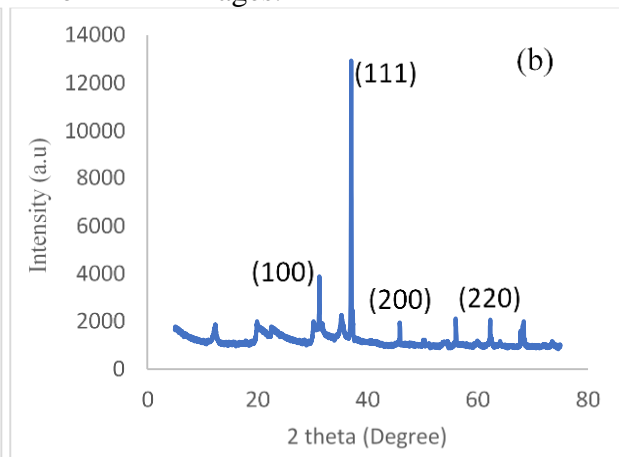


**Fig. 4a: XRD pattern of the AgNPs**

confirms the successful synthesis of AgNPs, while the presence of carbon and oxygen suggests the use of organic stabilizers or capping agents, likely to enhance nanoparticle stability and prevent agglomeration. The trace iron content might result from contamination during the synthesis process. Similarly, the EDS results for ZnNPs (zinc nanoparticles) indicate that the major compositions are zinc (40.9 wt%), carbon (41.5 wt%), and oxygen (17.6 wt%).

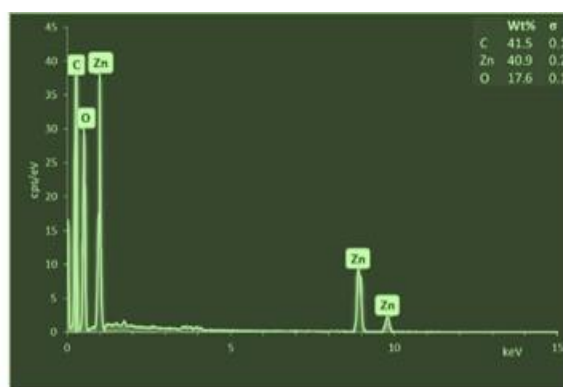


**Fig. 5b: EDS of ZnNPs**

likely due to a thicker organic coating or a more carbonaceous synthesis environment. In both cases, the EDS data validates the formation of nanoparticles with silver and zinc as the primary components, supported by the presence of organic and stabilizing elements. (Brown *et al.*, 2023; Ituen *et al.*, 2020).





#### 4.0 Conclusion

In this study, silver and zinc nanoparticles (AgNPs and ZnNPs) were successfully synthesized using the aqueous extract of *A. toxicaria* bark. The color changes observed during the synthesis process were indicative of the reduction of silver nitrate and zinc chloride into AgNPs and ZnNPs, respectively. The UV-Visible spectroscopy analysis revealed the characteristic surface plasmon resonance (SPR) peaks for both AgNPs and ZnNPs, confirming their successful formation. The FTIR analysis indicated the involvement of flavonoids and proteins in the reduction process, while SEM and TEM images provided insights into the morphology and size distribution of the nanoparticles. The XRD patterns confirmed the crystalline nature of the nanoparticles, with the AgNPs exhibiting a face-centered cubic (fcc) structure. Additionally, the EDS analysis showed the presence of silver and zinc in the nanoparticles, supporting the formation of the respective metal nanoparticles.

The results obtained from this study demonstrate the successful green synthesis of AgNPs and ZnNPs using *A. toxicaria* extract. The synthesis process is facilitated by the phytochemicals in the plant extract, which act as reducing and stabilizing agents. The nanoparticles exhibited promising characteristics such as well-defined crystalline structures, varied shapes, and distinct SPR peaks, making them suitable for various applications in catalysis, drug delivery, and environmental remediation.

It is recommended that further investigations be conducted to explore the potential applications of these nanoparticles, especially in fields like photocatalysis, environmental remediation, and biomedical applications. Additionally, optimizing the synthesis conditions could enhance the stability and uniformity of the nanoparticles, which could be crucial for scaling up their production for industrial applications. Future studies could

also focus on the toxicity assessment and biocompatibility of the synthesized nanoparticles to ensure their safe application in various sectors.

#### 5.0 References

- Adeyemi, J. O., Oriola, A. O., Onwudiwe, D. C. & Oyedeji, A. O. (2022). Plant extracts mediated metal-based nanoparticles: synthesis and biological applications. *Biomolecules*, 12, 5, p. 627.
- Adrianto, N., Panre, A. M., Istiqomah, N. I., Riswan, M., Apriliani, F. & Suharyadi, E. (2022). Localized surface plasmon resonance properties of green synthesized silver nanoparticles. *Nano-Structures & Nano-Objects*, 31, 100895.
- Afonso, I. S., Cardoso, B., Nobrega, G., Minas, G., Ribeiro, J. E. & Lima, R. A. (2024). Green synthesis of nanoparticles from olive oil waste for environmental and health applications: A review. *Journal of Environmental Chemical Engineering*, 114022.
- Ahmed, A., Singh, A., Padha, B., Sundramoorthy, A. K., Tomar, A. & Arya, S. (2022). UV-vis spectroscopic method for detection and removal of heavy metal ions in water using Ag-doped ZnO nanoparticles. *Chemosphere*, 303, p. 135208.
- Akpanudo, N. W., & Olabemiwo, O. M. (2024). Synthesis and characterization of silver nanoparticles and nanocomposites using *Echinochloa pyramidalis* (Antelope grass) plant parts and the application of the nanocomposite. *South African Journal of Chemical Engineering*, 4, 1, pp. 98–110.
- Alex, A. M., Subburaman, S., Chauhan, S., Ahuja, V., Abdi, G., & Abbasi Tarighat, M. (2024). Green synthesis of silver nanoparticles prepared with *Ocimum* species and assessment of anticancer potential. *Scientific Reports*, 14, 11707. <https://doi.org/10.1038/s41598-024-61946-y>.



- Ali, M. H., Azad, M. A. K., Khan, K. A., Rahman, M. O., Chakma, U. & Kumer, A. (2023). Analysis of crystallographic structures and properties of silver nanoparticles synthesized using PKL extract and nanoscale characterization techniques. *ACS omega*, 8, 31, pp. 28133-28142.
- Alsailawi, H. A., Mudhafar, M., Hanan, A. H., Ayat, S. S., Dhahi, S. J., Ruaa, K. M. & Raheem, H. A. (2023, September). Phytochemical screening and antibacterial activities of antiaris toxicaria stem, Polyalthia rumphii leaves and Polyalthia bullata stem extracts. In *AIP Conference Proceedings* (Vol. 2845, No. 1). AIP Publishing.
- Anandalakshmi, K., Venugobal, J. & Ramasamy, V. J. A. N. (2016). Characterization of silver nanoparticles by green synthesis method using *Petalium murex* leaf extract and their antibacterial activity. *Applied Nanoscience*, 6, pp. 399-408.
- Anandalakshmi, K., Venugobal, J., & Ramasamy, V. (2016). Characterization of silver nanoparticles by green synthesis method using *Petalium murex* leaf extract and their antibacterial activity. *Applied Nanoscience*, 6, 399-408. <https://doi.org/10.1007/s13204-015-0449-z>.
- Awwad, A. M., Salem, N. M., Aqarbeh, M. M. & Abdulaziz, F. M. (2020). Green synthesis, characterization of silver sulfide nanoparticles, and antibacterial activity evaluation. *Chem. Int*, 6, 1, pp. 42-48.
- Banjara, R. A., Kumar, A., Aneshwari, R., Satnami, M. L. & Sinha, S. K. (2024). A comparative analysis of chemical vs green synthesis of nanoparticles and their various applications. *Environmental Nanotechnology, Monitoring & Management*, 100988.
- Brown, H. K., El Haskouri, J., Marcos, M. D., Ros-Lis, J. V., Amorós, P., Úbeda Picot, M. Á. & Pérez-Pla, F. (2023). Synthesis and Catalytic Activity for 2, 3, and 4-Nitrophenol Reduction of Green Catalysts Based on Cu, Ag and Au Nanoparticles Deposited on Polydopamine-Magnetite Porous Supports. *Nanomaterials*, 13, 15, pp. 2162.
- Eddy, N. O., Edet, U. E., Oladele J. O., Kelle, H. I., Ogoko. E. C., Odiongenyi, A. O., Ameh, P., Ukpe, R. A., Ogbodo, R., Garg, R. and Garg, R. (2023). Synthesis and application of novel microporous framework of nanocomposite from trona for photocatalysed degradation of methyl orange dye. *Environmental Monitoring and Assessment*. DOI : 10.1007/s10661-023-12014-x.
- Eddy, N. O., Garg, R., Garg, R., Ukpe, R. A. and Abugu, H. (2023). Adsorption and photodegradation of organic contaminants by silver nanoparticles: isotherms, kinetics, and computational analysis. *Environmental Monitoring and Assessment*, DOI : 10.1007/s10661-023-12194-6,
- Eddy, N. O., Jibrin, J. I., Ukpe, R. A., Odiongenyi, A., Iqbal, A., Kasiemobi, A. M., Oladele, J. O., & Runde, M. (2024). Experimental and Theoretical Investigations of Photolytic and Photocatalysed Degradations of Crystal Violet Dye (CVD) in Water by oyster shells derived CaO nanoparticles (CaO-NP), *Journal of Hazardous Materials Advances*, 13, 100413, <https://doi.org/10.1016/j.hazadv.2024.100413>.
- Eddy, N. O., Oladede, J., Eze, I. S., Garg, R., Garg, R., & Paktin, H. (2024). Synthesis and characterization of CaO nanoparticles from periwinkle shell for the treatment of tetracycline-contaminated water by adsorption and photocatalyzed degradation. *Results in Engineering*, 103374. <https://doi.org/10.1016/j.rineng.2024.103374>.



- Ekwumemgbo, P. A. Gideon Adamu Shallangwa, G. A., Okon, I. E & Ibe Awodi, I. (2023). Green Synthesis and characterization of iron oxide nanoparticles using *Prosopis Africana* leaf extract. *Communication in Physical Sciences*, 9, 2, pp. 125-136.
- Essien, E. R., Atasie, V. N., Okefor, A. O. & Nwude, D. O. (2020). Biogenic synthesis of magnesium oxide nanoparticles using *Manihot esculenta* (Crantz) leaf extract. *International Nano Letters*, 10, 1, pp. 43–48.
- Fahim, M., Shahzaib, A., Nishat, N., Jahan, A., Bhat, T. A., & Inam, A. (2024). Green synthesis of silver nanoparticles: A comprehensive review of methods, influencing factors, and applications. *JCIS Open*, 16, 100125. <https://doi.org/10.1016/j.jciso.2024.100125>.
- Garg, R., Garg, R., Eddy, N. O., Almohana, A. I., Fahad, S., Khan, M. A. & Hong, S. H. (2022). Biosynthesized silica-based zinc oxide nanocomposites for the sequestration of heavy metal ions from aqueous solutions. *Journal of King Saud University-Science* <https://doi.org/10.1016/j.jksus.2022.101996>.
- Gopalakrishnan, S., Kaupa, P., Lakshmi, S. Y. S. & Banu, F. (2015). Antimicrobial activity of synthesized silver nanoparticles and phytochemical screening of the aqueous extract of *Antiaris toxicaria*. *Indian J. Drugs and Diseases*, 4, 1, pp. 1-4.
- Harun-Ur-Rashid, M., Jahan, I., Foyez, T. & Imran, A. B. (2023). Bio-inspired nanomaterials for micro/nanodevices: a new era in biomedical applications. *Micromachines*, 14, 9, p. 1786.
- Hossain, M. M., Hamza, A., Polash, S. A., Tushar, M. H., Takikawa, M., Piash, A. B., Dekiwadia, C., Saha, T., Takeoka, S., & Sarker, S. R. (2024). Green synthesis of silver nanoparticles using *Phyllanthus emblica* extract: Investigation of antibacterial activity and biocompatibility *in vivo*. *RSC Pharmaceutical Journal*, 1, 245–258. <https://doi.org/10.1039/D3PM00077J>.
- Islam, M. F., Islam, S., Miah, M. A. S., Huq, A. K. O., Saha, A. K., Mou, Z. J., Mondol, M. M. H., & Bhuiyan, M. N. I. (2024). Green synthesis of zinc oxide nanoparticles using *Allium cepa* L. waste peel extracts and its antioxidant and antibacterial activities. *Heliyon*, 10(3), e25430. <https://doi.org/10.1016/j.heliyon.2024.e25430>.
- Ituen, E., Ekemini, E., Yuanhua, L & Singh, A. (2020). Green synthesis of Citrus reticulata peels extract silver nanoparticles and characterization of structural, biocide, and anti-corrosion properties. *Journal of Molecular Structure*, 1207, p. 127819.
- Jamil, Y. M. S., Al-Hakimi, A. N., Al-Maydama, H. M. A., Almahwiti, G. Y., Qasem, A., & Saleh, S. M. (2024). Optimum green synthesis, characterization, and antibacterial activity of silver nanoparticles prepared from an extract of *Aloe fleurentinorum*. *International Journal of Chemical Engineering*. <https://doi.org/10.1155/2024/2804165>.
- Jose, R. A., Merin, D. D., Arulananth, T. S., & Shaik, N. (2022). Characterization analysis of silver nanoparticles synthesized from *Chaetoceros calcitrans*. *Journal of Nanomaterials*, 2022, Article ID 4056551, 15 pages. <https://doi.org/10.1155/2022/4056551>.
- Juma, M. W., Birech, Z., Mwenze, N. M., Ondieki, A. M., Maaza, M. & Mokhotjwa, S. D. (2024). Localized surface plasmon resonance sensing of Trenbolone acetate dopant using silver nanoparticles. *Scientific Reports*, 14, 1, p. 5721.
- Kpega, T. C., Habila, J. D., Okon, I. E. & Ekwumemgbo, P. A. (2023). Green



- synthesis and characterization of zinc oxide nanoparticles using *Corchorus olitorius* leaf extract. *Aceh International Journal of Science and Technology*, 2, 3, pp. 358-367. doi: 10.13170/aijst.12.3.34013.
- Naiel, B., Fawzy, M., Halmy, M. W. A., & Mahmoud, A. E. D. (2022). Green synthesis of zinc oxide nanoparticles using Sea Lavender (*Limonium pruinatum* L. Chaz.) extract: Characterization, evaluation of anti-skin cancer, antimicrobial, and antioxidant potentials. *Scientific Reports*, 12, 20370. <https://doi.org/10.1038/s41598-022-24805-2>.
- Nair, G. M., Sajini, T. & Mathew, B. (2022). Advanced green approaches for metal and metal oxide nanoparticles synthesis and their environmental applications. *Talanta Open*, 5, 100080.
- Odoemelam, S. A., Oji, E. O., Eddy, N. O., Garg, R., Garg, R., Islam, S., Khan, M. A., Khan, N. A. & Zahmatkesh, S. (2023). Zinc oxide nanoparticles adsorb emerging pollutants (glyphosate pesticide) from aqueous solution. *Environmental Monitoring and Assessment*, <https://doi.org/10.1007/s10661-023-11255-0>.
- Prasad, S. R., Teli, S. B., Ghosh, J., Prasad, N. R., Shaikh, V. S., Nazeruddin, G. M. & Shaikh, Y. I. (2021). A review on bio-inspired synthesis of silver nanoparticles: their antimicrobial efficacy and toxicity. *Engineered Science*, 16, pp. 90-128.
- Pungle, R., Nile, S. H. & Kharat, A. S. (2023). Green synthesis and characterization of *Solanum xanthocarpum* capped silver nanoparticles and its antimicrobial effect on multidrug-resistant bacterial (MDR) isolates. *Chemical Biology & Drug Design*, 101, 3, pp. 469-478.
- Punjabi, K., Mehta, S., Chavan, R., Chitalia, V., Deogharkar, D., & Deshpande, S. (2018). Efficiency of biosynthesized silver and zinc nanoparticles against multi-drug resistant pathogens. *Frontiers in Microbiology*, 9, 2207. <https://doi.org/10.3389/fmicb.2018.02207>.
- Rahman, G., Fazal, H., Ullah, A., Ahmad, S., Nadeem, T., Ahmad, M. & Farid, A. (2024). Empowering silver and copper nanoparticles through aqueous fruit extract of *Solanum xanthocarpum* for sustainable advancements. *Biomass Conversion and Biorefinery*, pp. 1-15.
- Richards, R., Richards, P. J. M. R. & Matthews, P. J. (2021). Barkcloth from the Solomon Islands in the George Brown Collection. *From Field to Museum—Studies from Melanesia in Honour of Robin Torrence*, pp. 245-258.
- Saputra, I. S., & Yulizar, Y. (2016). Biosynthesis and characterization of ZnO nanoparticles using the aqueous leaf extract of *Imperata cylindrica* L. *IOP Conference Series: Journal of Physics: Conference Series*, 755, 011001. <https://doi.org/10.1088/1742-6596/755/1/011001>.
- Shanmugam, J., Dhayalan, M., Savaas Umar, M. R., Gopal, M., Ali Khan, M., Simal-Gandara, J., & Cid-Samamed, A. (2022). Green synthesis of silver nanoparticles using *Allium cepa* var. *aggregatum* natural extract: antibacterial and cytotoxic properties. *Nanomaterials*, 12, 10, p. 1725.
- Sharma, D., Gulati, S. S., Sharma, N. & Chaudhary, A. (2022). Sustainable synthesis of silver nanoparticles using various biological sources and waste materials: A review. *Emergent Materials*, 5, 6, pp. 1649-1678.
- Sharma, N., Banerjee, S., Tomar, R. S. & Kaushik, S. (2021). Phytochemicals and Microbial Metabolites as Capping Agents in Nanoparticle Formulation and Its Implications in Agriculture. In *Nanotechnology in Sustainable Agriculture*, pp. 97-114, CRC Press.



Shreyash, N., Bajpai, S., Khan, M. A., Vijay, Y., Tiwary, S. K. & Sonker, M. (2021). Green synthesis of nanoparticles and their biomedical applications: a review. *ACS Applied Nano Materials*, 4, 11, pp. 11428-11457.

Singh, K., Nancy, Bhattu, M., Singh, G., Mubarak, N. M., & Singh, J. (2023). Light-absorption-driven photocatalysis and antimicrobial potential of PVP-capped zinc oxide nanoparticles. *Scientific Reports*, 13, 13886. <https://doi.org/10.1038/s41598-023-41103-7>.

Subiono, T. & Tavip, M. A. (2023). Qualitative and quantitative phytochemicals of leaves, bark, and roots of *Antiaris toxicaria* Lesch., a promising natural medicinal plant and source of pesticides. *Plant Science Today*, 10, 1, pp. 5-10.

Ying, S., Guan, Z., Ofoegbu, P. C., Clubb, P., Rico, C., He, F. & Hong, J. (2022). Green synthesis of nanoparticles: Current developments and limitations. *Environmental Technology & Innovation*, 26, p. 102336.

### **Acknowledgements**

We wish to sincerely appreciate the financial assistance granted us by the Tertiary Education Trust Fund (TETFUND) through the Management of the University of Uyo, Uyo for this research.

### **Compliance with Ethical Standards Declaration**

#### **Ethical Approval**

Not Applicable

#### **Competing interests**

The authors declare that they have no known competing financial interests

#### **Funding**

This project was sponsored by TETFund under Institutional Based Research (IBR).

#### **Authors' Contributions**

TNA, IBA and ASJ participated in the experimental aspect of the research. NS and SES interpreted characterization results. The manuscript for this paper was compiled by TNA, IBA and ASJ.

